Dr. 2403

ornl

ORNL/TM-7591

R-2714 MASTER

OAK RIDGE NATIONAL LABORATORY

UNION CARBIDE

Tearing Mode Stability of Tokamak Plasmas with Elliptical Cross Section

B. A. Carreras
J. A. Holmes
H. R. Hicks
V. E. Lynch

OPERATED BY
UNION CARBIDE CORPORATION
FOR THE UNITED STATES
DEPARTMENT OF ENERGY

CONTENTS

ABSTRACT

The effect of the ellipticity of the plasma cross section on tearing mode stability is investigated. The induced coupling between modes is shown to be destabilizing; however, the modification of the equilibrium tends to stabilize the tearing modes. The net effect depends on the manner in which the equilibrium is modified as the plasma cross-section shape is changed.

1. INTRODUCTION

In searching for high beta tokamak equilibria that are stable with respect to ideal magnetohydrodynamic (MHD) modes, the noncircular shape of the plasma cross section has proven to be a favorable factor [1,2]. Several tokamaks have incorporated this feature of noncircular plasma cross section. Because the occurrence of major tokamak disruptions has been correlated with the tearing mode instability [3-6], it is of interest to study the effect of the noncircularity of the plasma cross section on tearing mode stability. In this paper we investigate this effect in the framework of the resistive MHD model for the particular case of elliptical cross section.

In Section 2, the reduced set of resistive fluid equations is presented along with some details on their numerical solution. The numerical results are presented in Sections 3 and 4 for the $m = 1$ mode and $m > 1$ modes, respectively. An analysis of these results is given in Section 5, and the conclusions are presented in Section 6.

2. EQUATIONS

A cylindrical model of the tearing modes in which the plasma pressure is ignored ($\beta \lesssim \varepsilon^2$, where ε is the inverse of the aspect ratio) will be used in this investigation. From the resistive fluid equations two assumptions are made: (1) the coupling to compressional Alfvén waves (which keep the radial component of the force balance in equilibrium) is neglected, and hence the toroidal magnetic field B_z is unchanged by the tearing modes; and (2) the toroidal component of the fluid velocity is negligibly small. Then, the components of both the magnetic field and fluid flow velocities in the poloidal plane can be

represented in terms of stream functions, and the resistive MHD equations can be reduced, in dimensionless form, to [4,7]

$$\frac{\partial \Psi}{\partial t} = -\vec{B} \cdot \vec{\nabla}\Phi + \eta J_\zeta - E^W_\zeta \,, \tag{1}$$

$$\frac{\partial U}{\partial t} + \vec{v}_\perp \cdot \vec{\nabla}_\perp U = -S^2 \vec{B} \cdot \vec{\nabla} J_\zeta \,. \tag{2}$$

In Eqs (1) and (2), the time is normalized to the resistive diffusion time, $\tau_R \equiv a^2 \mu_o / \eta_o$, and the lengths are normalized to a, the geometrical mean of the major axis b_o and minor axis a_o of the ellipse. The toroidal current density $J_\zeta = \vec{\nabla}^2_\perp \Psi$, the magnetic field $\vec{B} = -\varepsilon \vec{\nabla}_\perp \Psi \times \hat{\zeta} + \hat{\zeta}$, and the toroidal component of the vorticity $U = \vec{\nabla}^2_\perp \Phi$ are normalized to $B_z/\mu_o R_o$, B_z, and $B_z \tau_R^{-1}$, respectively. The resistivity η has been normalized to its value η_o at the magnetic axis. Here, $\zeta \equiv z/2\pi R_o$ is the normalized longitudinal cylindrical coordinate that represents the toroidal angle. In Eq. (2), $\vec{v}_\perp = \vec{\nabla}_\perp \Phi \times \hat{\zeta}$ is the poloidal fluid velocity; the subscript $\perp$ means perpendicular to the $\hat{\zeta}$ direction; and the quantity S is defined by $S \equiv \tau_R/\tau_{Hp}$, where τ_{Hp} is the poloidal Alfvén time $R_o(\mu_o \rho_m)^{1/2}/B_z$ (the mass density ρ_m is assumed to be constant).

Equations (1) and (2) have been expressed in equilibrium flux coordinates ρ, θ, ζ. The coordinate ρ labels the flux surfaces. In the circular cross-section limit ρ becomes the cylindrical radial coordinate r. The poloidal angle coordinate θ has been defined to make the equilibrium magnetic field lines straight. In the cylindrical limit, these coordinates are the same as the ones used in Ref. [8]. The effect of deforming the plasma cross section enters Eqs (1) and (2)

essentially through the $\vec{\nabla}_\perp^2$ operator, which can be expressed in this coordinate system as

$$\vec{\nabla}_\perp^2 f = \frac{1}{\rho}\frac{\partial}{\partial\rho}\left(\rho g^{\rho\rho}\frac{\partial f}{\partial\rho} + g^{\rho\theta}\frac{\partial f}{\partial\theta}\right) + \frac{1}{\rho}\frac{\partial}{\partial\theta}\left(g^{\rho\theta}\frac{\partial f}{\partial\rho} + \frac{g^{\theta\theta}}{\rho}\frac{\partial f}{\partial\theta}\right) ,$$

where $g^{\rho\rho}$, $g^{\rho\theta}$, and $g^{\theta\theta}$ are the components of the metric tensor.

To numerically advance Eqs (1) and (2), an initial value code RST has been employed. The RST code is a generalization of RSF [9] that is adequate to deal with more general coordinates. The noncircular cross-section equilibria are calculated by the fixed boundary code RSTEQ [10] and are given as input to RST.

A linear boundary value code has also been developed using a Δ' formalism (a Δ' solver). This allows a better interpretation of some of the results from the initial value code, verifies these results, and allows more efficient linear calculations. This has been done in a way analogous to the toroidal Δ' solver (TORDEL) described in Ref. [8]. Since the coordinate system is very well suited to tearing modes, only the coupling to two other poloidal Fourier components ($m \pm 2$) is necessary for each circularly unstable mode m. This holds even for ellipticities as large as $e = 2$ ($e \equiv b_o/a_o$). Figure 1 shows the distribution of magnetic energy among the Fourier components of an $n = 2$ tearing mode for different values of the ellipticity e. In this particular example the ($m = 3$; $n = 2$) tearing mode is unstable for a circular cylinder. The magnetic energy of the different components is normalized to the magnetic energy of the (3;2) component. The energy falloff of the side bands is exponential, and numerical tests have

verified that the contribution of the components with poloidal numbers $m \pm 4$ is negligible.

3. STABILITY OF THE (m = 1; n = 1) TEARING MODE

Edery et al. [11] have shown that the stability of the ideal, internal, m = 1 kink mode is sensitive to small distortions of a circular cylindrical equilibrium. In particular, they have proven that ellipticity is a destabilizing effect. Therefore, we expect that the linear growth rate of the m = 1 tearing mode will be enhanced with ellipticity, at least when the resistivity is small enough. We have investigated this effect with the initial value code. For a particular equilibrium q profile,

$$q(\rho) = q(0)\left[1 + (\rho/\rho_o)^{2\lambda}\right]^{1/\lambda} , \qquad (3)$$

with $q(0) = 0.65$, $\lambda = 2$, and $\rho_o = 0.46$, we have calculated the linear eigenvalue and eigenfunction for several values of the resistivity. Figure 2 shows the comparison between the linear growth rates for a circular cross-section cylinder and the corresponding ones for e = 1.7. The calculations were done for values of S ranging between 10^5 and 10^8 for the circular cross-section case. The results are plotted in Fig. 2 as a function of $S^{-1/3}$, the predicted scaling for the m = 1 tearing mode in cylindrical geometry. For a circular cross-section cylinder the growth rate goes to zero as S goes to infinity. This agrees with the fact that the ideal internal kink mode is marginally stable. For the elliptical cross section (e = 1.7), the calculation was repeated for the same sequence of values of S. The linear growth rate departs

from the $S^{-1/3}$ scaling, typical of the tearing mode, and does not go to zero as S goes to infinity. In this case it was possible to use the initial value code as an ideal MHD code by neglecting the ηJ_ζ term in Eq. (1). The growth rate obtained in this limit agrees with the trend shown by the decreasing resistivity values. These numerical results are consistent with the analytical predictions of Ref. [11]. For values of the resistivity such that $S \leq 10^6$, the linear growth rate of the (m = 1; n = 1) mode is slightly increased by ellipticity. It is necessary to go to values of S above 10^7 to see a strong destabilizing effect.

4. STABILITY OF TEARING MODES WITH m > 1

To numerically study the effect of the ellipticity on tearing mode stability, it is necessary to specify first how the plasma equilibrium is changed with increasing e. There are several ways of doing this, depending on what parameters are held constant while the shape of the plasma cross section is changed. In this paper, results will be presented for two alternative ways of modifying the equilibrium that are characterized as follows:

(1) Constant-q sequence. The safety factor q profile, S, and the total plasma volume are fixed as e increases. The toroidal current density profile and the resistivity profile change as a consequence of the change in the plasma cross section.

(2) Constant-J_ζ sequence. The current density profile, S, q(0), and the plasma volume remain fixed in this scanning. Therefore, the position of the singular surfaces relative to the current density and resistivity profiles changes as $q(\rho)$ changes.

In both sequences the modifications of the equilibrium with increasing ellipticity are particularly important near the plasma edge. For instance, q(1) goes from 3.1 to 5.6 in the constant-J_ζ sequence when the ellipticity increases from 1 to 2, as shown by the dashed line in Fig. 3. For the constant-q sequence the current density increases near the plasma edge and flattens the current gradient in this region. These equilibrium effects and the effect of the additional couplings between modes having the same toroidal number combine to make it difficult to predict the total effect on tearing mode stability. This combination also complicates the analysis of the results of the initial value code.

All the results of this section correspond to equilibria with a safety factor q profile larger than one. In this way the effect of the ideal, internal kink mode is excluded.

Figure 3 shows the linear growth rate of the n = 1 mode for a constant-J_ζ sequence of equilibria. The toroidal current density for these equilibria is parameterized as

$$J_\zeta(\rho) = -\frac{2}{q(0)} \frac{1}{\left[1 + (\rho/\rho_o)^{2\lambda}\right]^{1/\lambda+1}} , \qquad (4)$$

with q(0) = 1.08, λ = 4, ρ_o = 0.59, and S = 10^4 fixed. The linear growth rate increases with increasing ellipticity; however, the rate of increase noticeably diminishes as e approaches 2.

For a constant-q sequence of equilibria, the linear growth rates of the n = 1 and n = 2 modes are plotted in Fig. 4a. These equilibrium sequences have a safety factor q profile given by Eq. (3). Several

sequences of such equilibria have been studied, which correspond to different values of λ. For these sequences $q(0) = 1.34$, and $q(1) = 4.0$. The value of S for the results plotted in Fig. 4 is 10^4. For these sequences the linear growth rate of the tearing modes decreases with increasing ellipticity, particularly for the n = 1 mode. The n = 2 mode is weakly affected. The stabilizing effect of the ellipticity for this type of sequence is also reflected in the slight decrease of the saturated island widths for the 2/1 and 3/2 helicities (see Fig. 4b).

5. ANALYSIS OF THE NUMERICAL RESULTS

To better understand the previous results, a Δ' solver has been developed that, together with the initial value code, allows a detailed study of the linear stability problem. It is possible to separate the effects due to the modification of the equilibrium from the effect of the coupling between the different Fourier components of the eigenmode. By separating the equilibrium quantities from the perturbed ones,

$$\Psi(\rho,\Theta,\zeta,t) = \psi_{eq}(\rho) + \tilde{\Psi}(\rho,\Theta,\zeta,t) ,$$

it is possible to linearize Eqs (1) and (2). It is clear in this case that the time dependence and the dependence on the toroidal angular variable are factorizable. For a given n value, the corresponding eigenfunction can be expanded in Fourier series in the poloidal angle:

$$\tilde{\psi}_n(\rho,\Theta) = \sum_m \psi_{mn}(\rho)\cos m\Theta . \qquad (5)$$

Ellipticity only couples poloidal modes with the same parity.

Therefore, the summation in Eq. (5) extends over either even or odd m values.

In the linearized equations one can neglect resistivity and inertia outside the singular layers. It is also assumed that for each (m; n) mode that is unstable in circular cross section, only two side bands (m ± 2; n) are required to describe a full eigenmode in the elliptical case. This is a result of a judicious choice of coordinate system, pointed out in Section 2 and verified with initial value calculations. Having taken these points into account, it is easy to derive a coupled system of differential equations for the three Fourier components of the poloidal flux:

$$\left(\frac{m}{\rho}\frac{d\psi_{eq}}{d\rho} + n\right)\left\{\frac{1}{\rho}\frac{d}{d\rho}\left(\rho g_o^{\rho\rho}\frac{d\psi_{mn}}{d\rho}\right) - g_o^{\theta\theta}\frac{m^2}{\rho^2}\psi_{mn} + \frac{1}{2}\left[\frac{1}{\rho}\frac{d}{d\rho}\left(\rho g_2^{\rho\rho}\frac{d\psi_{m-2;n}}{d\rho}\right)\right.\right.$$

$$\left. + \frac{2(m-1)}{\rho} g_2^{\rho\theta}\frac{d\psi_{m-2;n}}{d\rho} + \frac{m-2}{\rho}\left(\frac{dg_2^{\rho\theta}}{d\rho} - \frac{m}{\rho} g_2^{\theta\theta}\right)\psi_{m-2;n}\right]$$

$$+ \frac{1}{2}\left[\frac{1}{\rho}\frac{d}{d\rho}\left(\rho g_2^{\rho\rho}\frac{d\psi_{m+2;n}}{d\rho}\right) - \frac{2(m+1)}{\rho} g_2^{\rho\theta}\frac{d\psi_{m+2;n}}{d\rho}\right.$$

$$\left.\left. - \frac{m+2}{\rho}\left(\frac{dg_2^{\rho\theta}}{d\rho} + \frac{m}{\rho} g_2^{\theta\theta}\right)\psi_{m+2;n}\right]\right\}$$

$$= \frac{m}{\rho}\frac{d}{d\rho}\left[\frac{1}{\rho}\frac{d}{d\rho}\left(\rho g_o^{\rho\rho}\frac{d\psi_{eq}}{d\rho}\right)\right]\psi_{mn} , \qquad (6)$$

$$\left(\frac{m-2}{\rho}\frac{d\psi_{eq}}{d\rho} + n\right)\left\{\frac{1}{\rho}\frac{d}{d\rho}\left(\rho g_o^{\rho\rho}\frac{d\psi_{m-2;n}}{d\rho}\right) - g_o^{\theta\theta}\frac{(m-2)^2}{\rho^2}\psi_{m-2;n}\right.$$

$$+ \frac{1}{2}\left[\frac{1}{\rho}\frac{d}{d\rho}\left(\rho g_2^{\rho\rho}\frac{d\psi_{mn}}{d\rho}\right) - \frac{2(m-1)}{\rho} g_2^{\rho\theta}\frac{d\psi_{mn}}{d\rho}\right.$$

$$- \frac{m}{\rho}\left(\frac{dg_2^{\rho\Theta}}{d\rho} + \frac{m-2}{\rho} g_2^{\Theta\Theta}\right)\psi_{mn}\Big]\Big\}$$

$$= \frac{m-2}{\rho}\frac{d}{d\rho}\left[\frac{1}{\rho}\frac{d}{d\rho}\left(\rho g_o^{\rho\rho}\frac{d\psi_{eq}}{d\rho}\right)\right]\psi_{m-2;n} \,, \qquad (7)$$

$$\left(\frac{m+2}{\rho}\frac{d\psi_{eq}}{d\rho} + n\right)\left\{\frac{1}{\rho}\frac{d}{d\rho}\left(\rho g_o^{\rho\rho}\frac{d\psi_{m+2;n}}{d\rho}\right) - g_o^{\Theta\Theta}\frac{(m+2)^2}{\rho^2}\psi_{m+2;n}\right.$$

$$+ \frac{1}{2}\left[\frac{1}{\rho}\frac{d}{d\rho}\left(\rho g_2^{\rho\rho}\frac{d\psi_{mn}}{d\rho}\right) + \frac{2(m+1)}{\rho} g_2^{\rho\Theta}\frac{d\psi_{mn}}{d\rho}\right.$$

$$\left.\left. + \frac{m}{\rho}\left(\frac{dg_2^{\rho\Theta}}{d\rho} - \frac{m+2}{\rho} g_2^{\Theta\rho}\right)\psi_{mn}\right]\right\}$$

$$= \frac{m+2}{\rho}\frac{d}{d\rho}\left[\frac{1}{\rho}\frac{d}{d\rho}\left(\rho g_o^{\rho\rho}\frac{d\psi_{eq}}{d\rho}\right)\right]\psi_{m+2;n} \,. \qquad (8)$$

The derivation is totally analogous to the one described for toroidal geometry in Ref. [8]. Thus, the details are omitted here.

In Eqs (6), (7), and (8), $g_\ell^{\rho\rho}$, $g_\ell^{\rho\Theta}$, and $g_\ell^{\Theta\Theta}$ are the ℓ-th Fourier components of the elements of the metric tensor.

As in Ref. [8], solving the linearized equations inside the singular layers gives the matching conditions across the singularities. As a result, Eqs (6), (7), and (8) can be solved as a boundary value problem, and a computer code that solves these equations has been written. The numerical scheme is analogous to the one described in Ref. [8].

The Δ' solver has been used to find the eigenfunction and eigenvalue of an n = 1 tearing mode. For the equilibria considered in the previous section, the (m = 2; n = 1) mode is the only unstable n = 1 mode in the circular cross-section limit. Therefore, only the

(0;1) and (4;1) Fourier components, together with the (2;1), are included in the calculation. The (4;1) component is the most sensitive one to the approximations made and to the numerical method used. The (0;1) component can be simply obtained by quadrature. Hence, it is a good test of our calculation to compare the (4;1) component with the results of the initial value code (see Fig. 5). The agreement is excellent.

It is possible to analyze the numerical results presented in the previous section and to unravel the seeming contradiction between the results of the two types of equilibrium sequences.

Figure 6a shows a comparison of the linear growth rates obtained with the Δ' solver and the initial value code for a constant-q type of sequence with $\lambda = 1.75$, $q(0) = 1.34$, and $q(1) = 4$. The growth rates have been normalized to their value for $e = 1$ in order to show the percentage change with ellipticity. The results from both codes agree well. The Δ' solver can now be used to calculate the change of Δ' due to the change of the toroidal current density when the ellipticity increases. This can be done by neglecting the (0;1) and (4;1) contributions in Eq. (6). This equation becomes equal to the equation for a circular cylinder except for the $g_0^{\rho\rho}$ term in the toroidal current density. This term gives the measure of the equilibrium deformation and, in the particular case considered here, gives a strong stabilization when ellipticity increases (see Fig. 6b). When the coupling to the (0;1) and (4;1) components is included, Δ' increases. However, for this particular equilibrium sequence, the destabilizing effect due to the poloidal coupling is weaker than the stabilizing effect due to the decrease in the equilibrium current gradient at the

q = 2 rational surface. Thus, the overall effect is stabilizing. (There is also an effect brought about by the modification of the resistivity profile. However, this effect is less important than either of the other effects, and we shall not discuss it here.)

Both effects (mode coupling and deformation) are also present for a constant-J_ζ equilibrium sequence. The coupling between additional poloidal modes is once again a destabilizing effect. The modification of the equilibrium due to the increase in the ellipticity corresponds to an increase in the values of q near the plasma edge. Consequently, the resonant surfaces move toward the inside of the plasma, which gives a stabilizing effect. For the constant-J_ζ sequence considered before (Fig. 3), the equilibrium effects are weaker than the coupling effect, and the result is a destabilization of the tearing mode.

It is important to remark that in this section the change of the linear growth rates has been interpreted as simply a Δ' effect. This is true since the inside tearing layer contributions due to ellipticity are negligible compared with the change of Δ'.

A particular case of interest occurs when, for a given n value, there is a single resonant surface in the plasma. For this situation an analytic determination of the change of Δ' due to the coupling induced by ellipticity can be made. It is then possible to prove the destabilizing character of this effect. For this particular case, one expects that each sideband of the (m;n) resonant component has a similar effect on the stability of the mode, and numerical results support this assumption. Therefore, the calculation can be reduced to include only one sideband; namely, for the n = 1 mode it is enough to consider the (2;1) and (0;1) components. The calculation can be

carried out analytically if the ellipticity is close to 1. It is then possible to do a perturbation expansion in the parameter $\delta \equiv (e^2 - 1)/(e^2 + 1)$. The eigenfunctions are

$$\psi_{mn}(\rho) = \sum_{k=0}^{\infty} \delta^k \psi_{mn}^{(k)}(\rho) \ .$$

It is assumed that the zero order term is nonzero only for the (2;1) component and equal to the eigenfunction of a circular cross-section cylinder with the same q-profile and toroidal current density as the case considered.

In Eqs (6), (7), and (8), the $g_2^{\rho\rho}$, $g_2^{\rho\theta}$, and $g_2^{\theta\theta}$ terms are of order δ. To make that explicit, we can multiply them by δ and, at the end of the calculation, set $\delta = 1$. Due to this ordering the first order contribution to the (2;1) component is zero. The first order effect consists in generating the (0;1) component, which can be easily calculated using Eq. (7). The result is

$$\psi_{01}^{(1)}(\rho) = \begin{cases} \psi_{01}^{(1)}(0) - \int_0^{\rho} A(\rho')d\rho' & 0 \leq \rho < \rho_{21} \ , \\ \int_{\rho}^{1} A(\rho')d\rho' & \rho_{21} < \rho \leq 1 \ , \end{cases} \tag{9}$$

where ρ_{21} is the position of the q = 2 singular surface,

$$\psi_{01}^{(1)}(0) = \int_0^1 d\rho' A(\rho') \tag{10}$$

and

$$A(\rho) \equiv \left[g_2^{\rho\rho} \frac{d\psi_{21}^{(0)}}{d\rho} - g_2^{\rho\theta} \psi_{21}^{(0)} \right] / \rho g_o^{\rho\rho} \tag{11}$$

Now it is possible to calculate the second order effect on the (2;1) component by substituting Eq. (9) into Eq. (6), keeping only δ^2 terms. This equation can be solved formally giving a simple expression for Δ'_{21} including terms up to second order:

$$\Delta'_{21} = \Delta'^{(0)}_{21} \left\{ 1 + \frac{1}{4} \left[\frac{g_2^{\rho\rho}(\rho_{21})}{g_o^{\rho\rho} \rho_{21}} \right]^2 \right\}$$

$$+ \frac{1}{4\rho_{21} g_o^{\rho\rho}(\rho_{21}) \left[\psi_{21}^{(0)}(\rho_{21}) \right]^2} \int_0^1 \rho \, d\rho \left\{ \frac{(g_2^{\rho\rho})^2}{2 g_o^{\rho\rho}} \left[\frac{d\psi_{21}^{(0)}}{d\rho} \right]^2 \right.$$

$$\left. + \frac{1}{\rho^2} \left[\frac{d}{d\rho} \left(\frac{g_2^{\rho\rho} g_2^{\rho\theta}}{g_o^{\rho\rho}} \right) + \frac{2 g_2^{\rho\theta}}{\rho g_o^{\rho\rho}} \right] (\psi_{21}^{(0)})^2 \right\} \tag{12}$$

In this expression δ has already been set to 1, and $\Delta'^{(0)}_{21}$ is the Δ' for the zero order solution, including the effect of the change of the equilibrium induced by ellipticity. It can be shown from Eq. (12) that the coupling between Fourier components of a linear eigenmode is destabilizing.

6. CONCLUSIONS

The ellipticity of the plasma cross section can affect the stability of a tearing mode in two ways: (1) by modifying the equilibrium and (2) by coupling modes having the same toroidal mode number n and poloidal mode numbers with the same parity. This second

effect is always destabilizing, whereas the first one is, in general, stabilizing. It is necessary to study each case individually to determine the net effect.

ACKNOWLEDGMENTS

We are grateful to W. A. Cooper for carefully reading this manuscript. One of us (B.A.C.) wishes to thank M. N. Bussac for fruitful discussions. We also acknowledge D. K. Lee for implementing the Δ' solver code.

This research was sponsored by the Office of Fusion Energy, U.S. Department of Energy, under contract W-7405-eng-26 with the Union Carbide Corporation.

REFERENCES

[1] TODD, A. M. M., MANICKAM, J., OKABAYASHI, M., CHANCE, M. S., GRIMM, R. C., GREEN, J. M., JOHNSON, J. L., Nucl. Fusion 19 (1979) 743.

[2] CHARLTON, L. A., NELSON, D. B., DORY, R. A., Phys. Rev. Lett. 45 (1980) 24.

[3] WADDELL, B. V., CARRERAS, B., HICKS, H. R., HOLMES, J. A., LEE, D. K., Phys. Rev. Lett. 41 (1978) 1383.

[4] CARRERAS, B., HICKS, H. R., HOLMES, J. A., WADDELL, B. V., Nonlinear Coupling of Tearing Modes with Self-Consistent Resistivity Evolution, Oak Ridge National Laboratory Report ORNL/TM-7161 (1980), to be published in Phys. Fluids.

[5] WHITE, R. B., MONTICELLO, D. A., ROSENBLUTH, M. N., Phys. Rev. Lett. 39 (1977) 1678.

[6] TOI, K., ITOH, S., KADOTA, K., KAWAHATA, K., NODA, N., SAKWAI, K., SATO, K., TANAHASHI, S., YASUE, S., Nucl. Fusion 19 (1979) 1643; McGUIRE, K. M., ROBINSON, D. C., Major Disruptions in the Tosca Tokamak, Culham Laboratory Report CLM P-601 (1980).

[7] STRAUSS, H. R., Phys. Fluids 19 (1976) 134.

[8] CARRERAS, B., HICKS, H. R., LEE, D. K., Effect of the Toroidal Coupling on the Stability of Tearing Modes, Oak Ridge National Laboratory Report ORNL/TM-7281 (1980), to be published in Phys. Fluids.

[9] HICKS, H. R., CARRERAS, B., HOLMES, J. A., LEE, D. K., WADDELL, B. V., 3-D Nonlinear Calculations of Resistive Tearing Modes, Oak Ridge National Laboratory Report ORNL/TM-7132, to be published.

[10] HOLMES, J. A., PENG, Y-K. M., LYNCH, S. J., J. Comput. Phys. 36 (1980) 35.

[11] EDERY, D., LAVAL, G., PELLAT, R., SOULÉ, J. L., Phys. Fluids 19 (1976) 260.

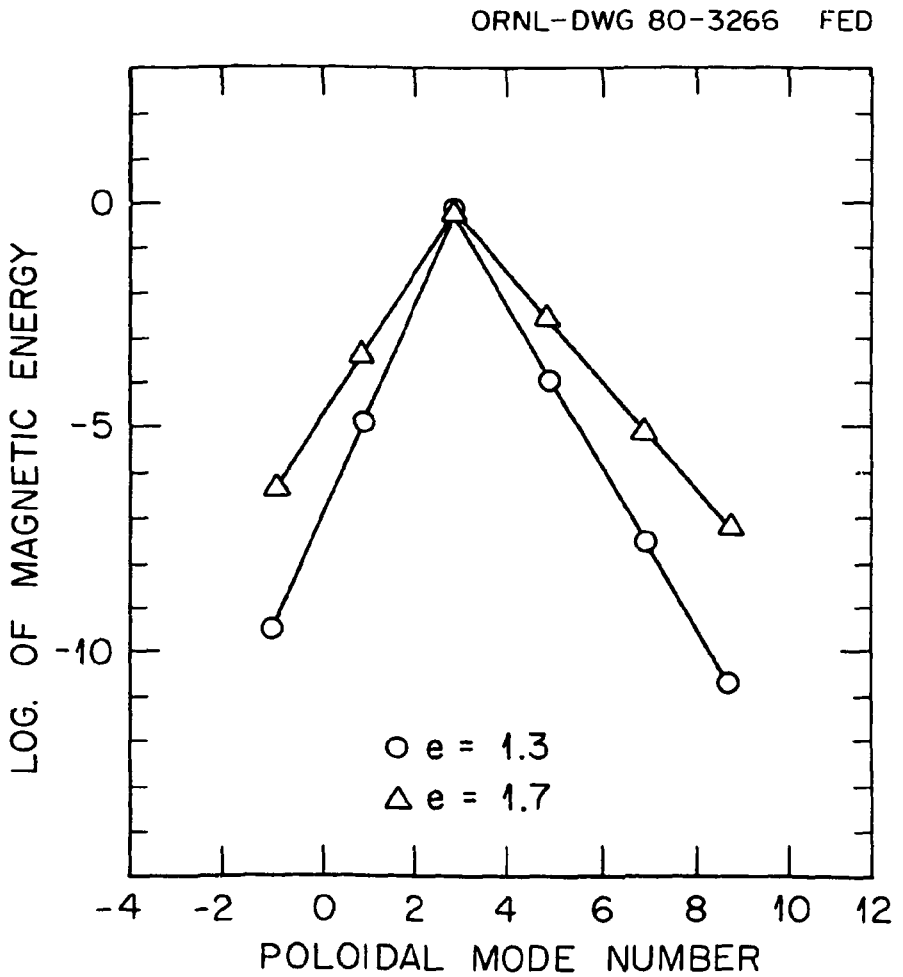
ORNL-DWG 80-3266 FED
LOG. OF MAGNETIC ENERGY
0
-5
-10
-4
-2
0
2
4
6
8
10
12
POLOIDAL MODE NUMBER
O e = 1.3
Δ e = 1.7

Fig. 1

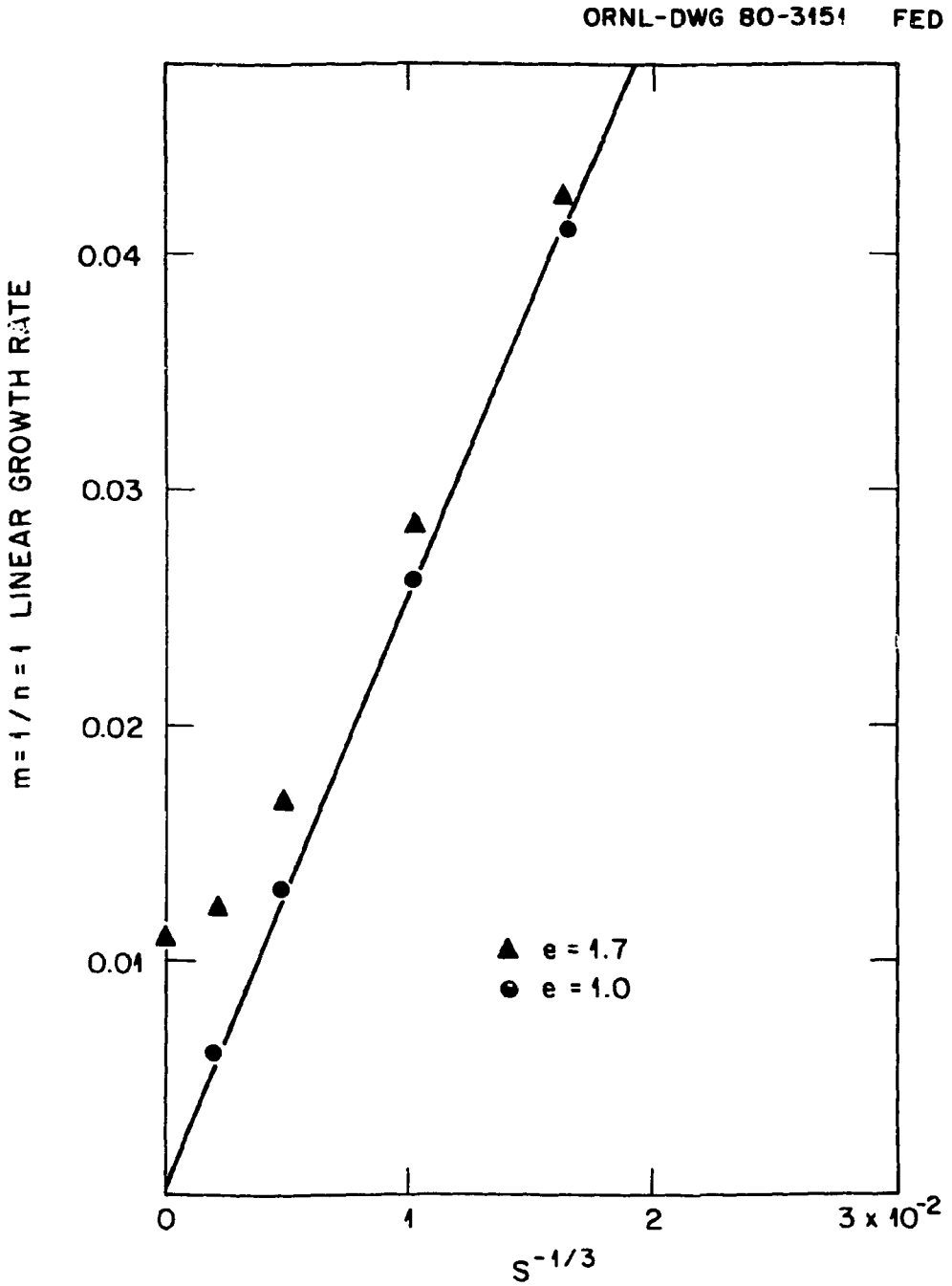
ORNL-DWG 80-3151 FED
m = 1 / n = 1 LINEAR GROWTH RATE
0.04
0.03
0.02
0.01
0
1
2
3 x 10^-2
S^-1/3
e = 1.7
e = 1.0

Fig. 2

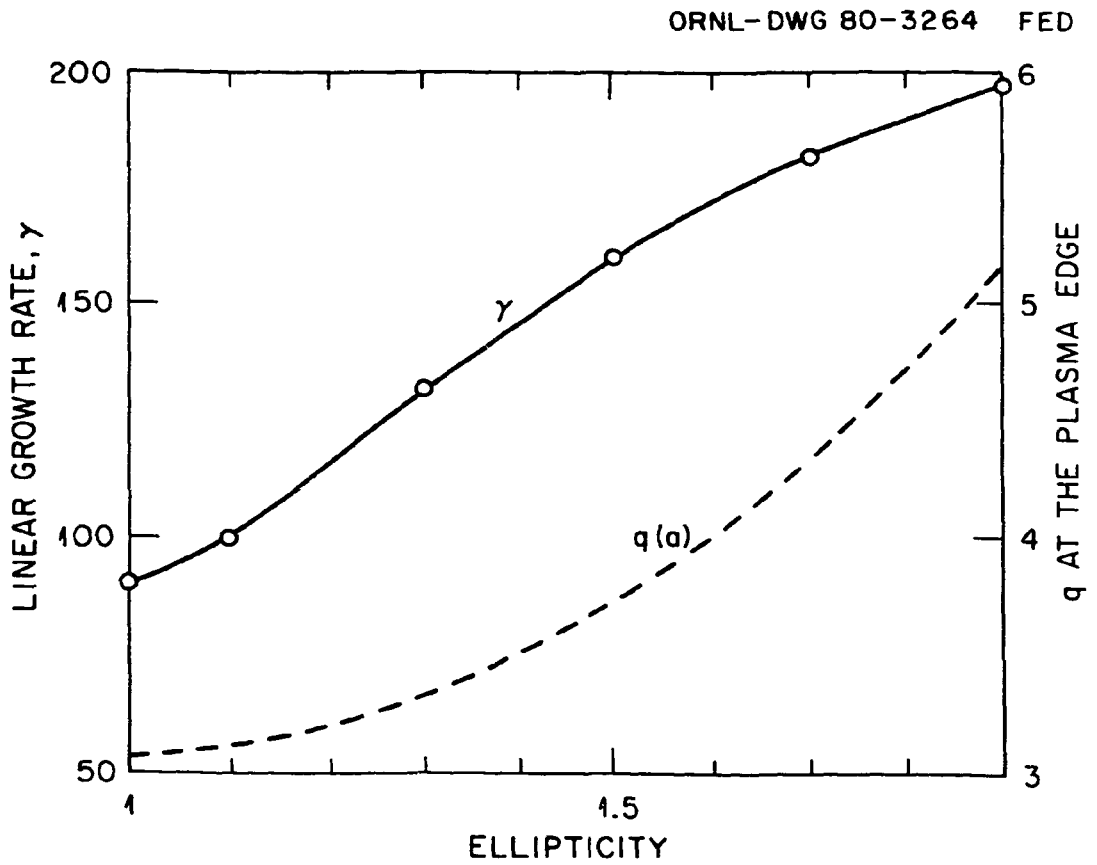
ORNL-DWG 80-3264 FED
200
150
100
50
LINEAR GROWTH RATE, γ
γ
q(a)
6
5
4
3
q AT THE PLASMA EDGE
1
1.5
ELLIPTICITY

Fig. 3

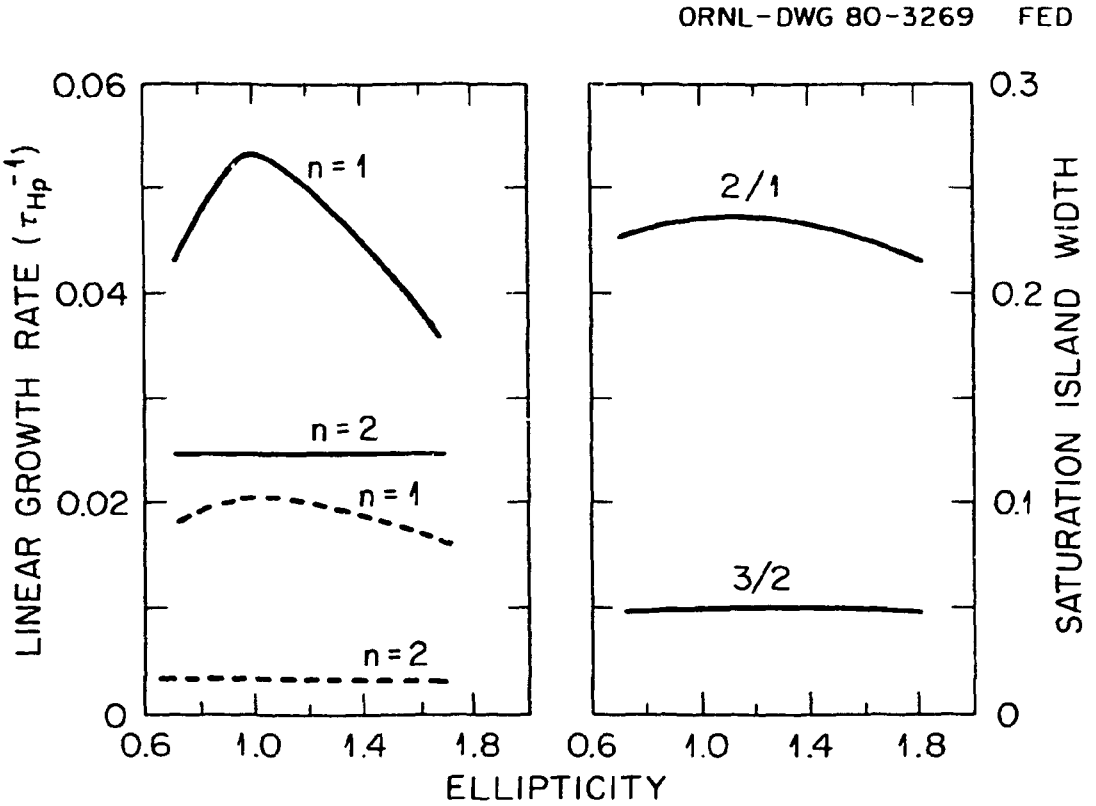
ORNL-DWG 80-3269 FED
0.06
0.04
0.02
0
LINEAR GROWTH RATE (τ_{Hp}^{-1})
n = 1
n = 2
n = 1
n = 2
0.3
0.2
0.1
0
SATURATION ISLAND WIDTH
2/1
3/2
0.6
1.0
1.4
1.8
0.6
1.0
1.4
1.8
ELLIPTICITY

Fig. 4

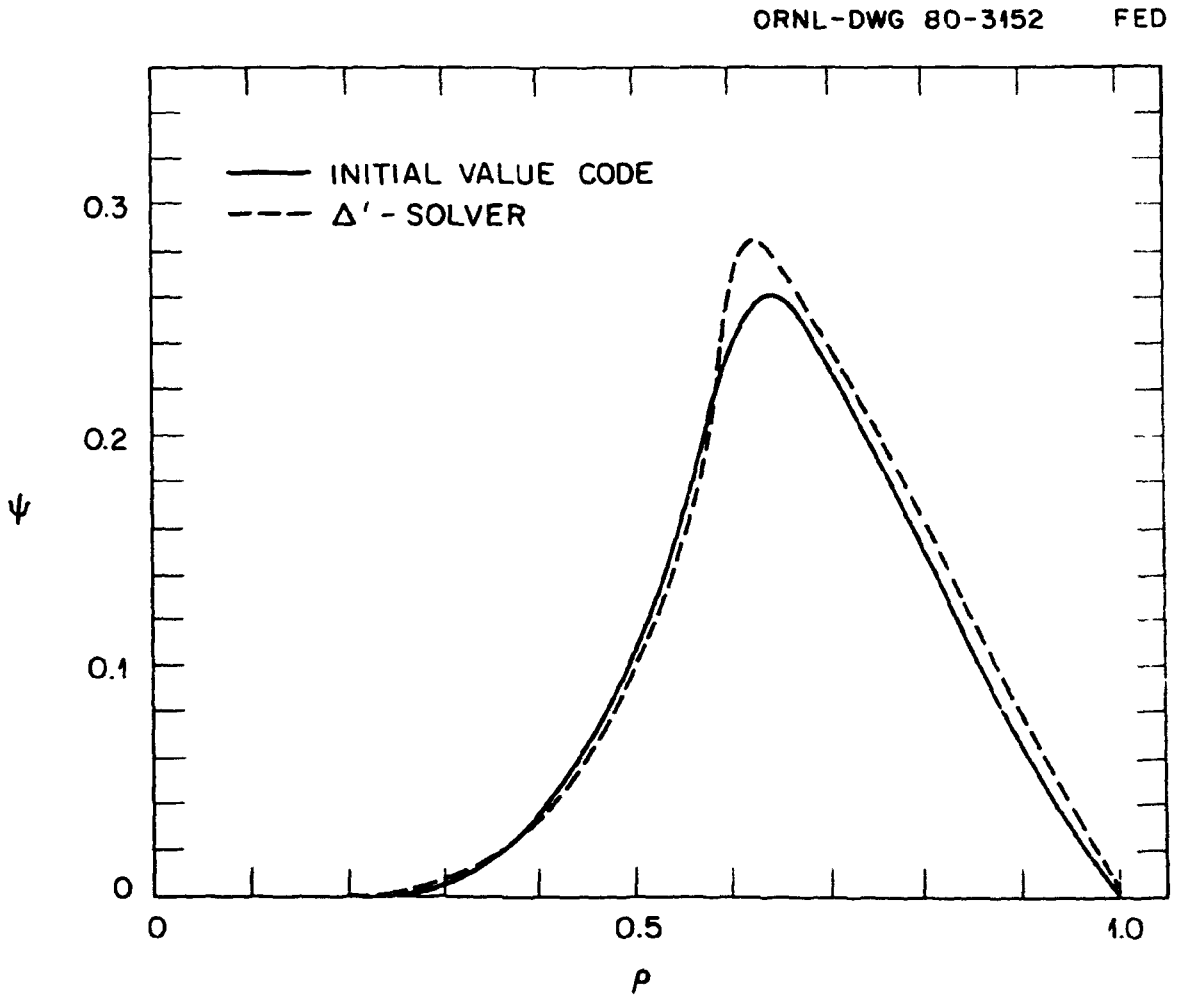
ORNL-DWG 80-3152 FED
INITIAL VALUE CODE
Δ' - SOLVER
0.3
0.2
0.1
0
ψ
0
0.5
1.0
ρ

Fig. 5

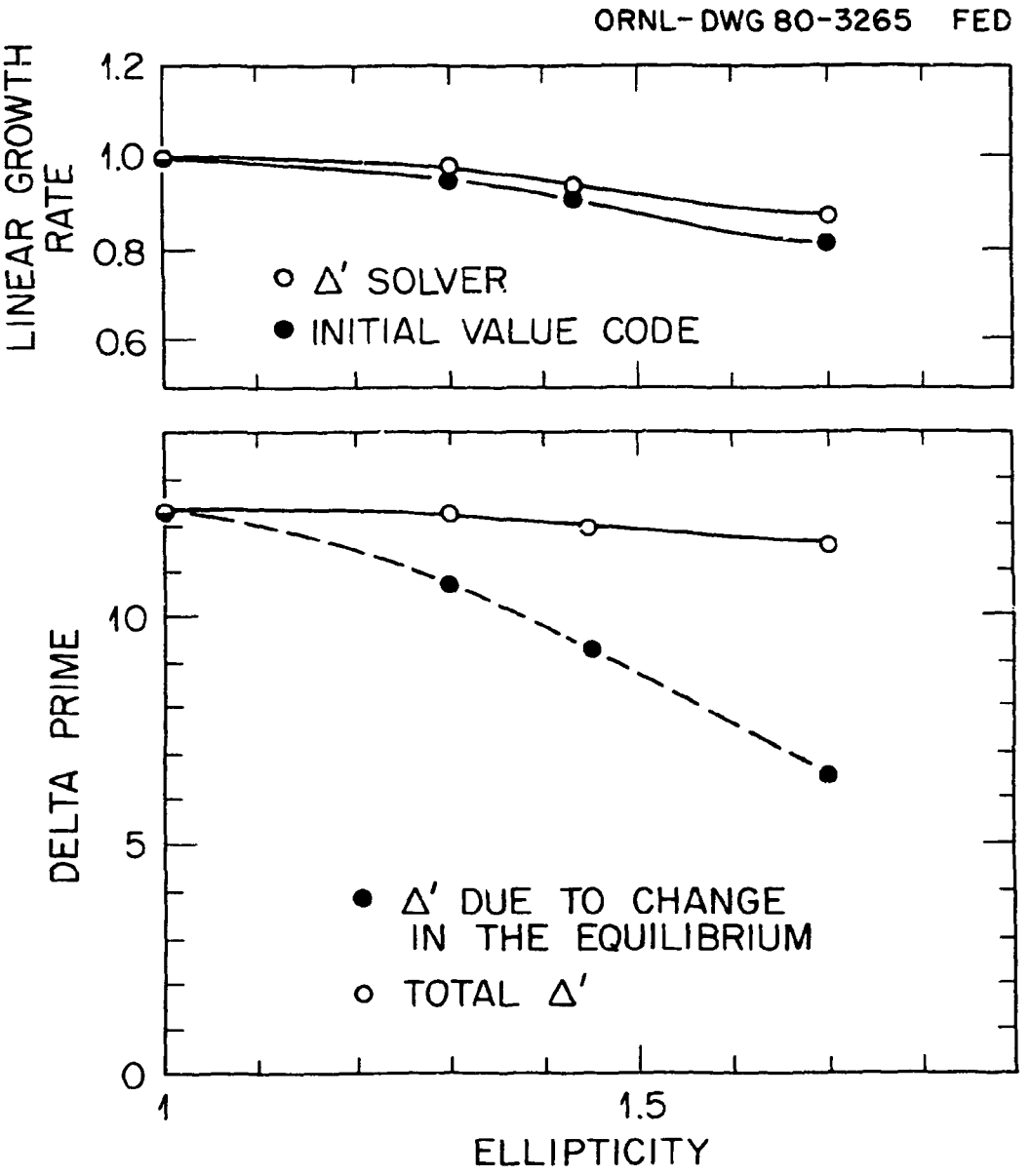
ORNL-DWG 80-3265 FED
LINEAR GROWTH RATE
1.2
1.0
0.8
0.6
Δ′ SOLVER
INITIAL VALUE CODE
DELTA PRIME
10
5
0
Δ′ DUE TO CHANGE IN THE EQUILIBRIUM
TOTAL Δ′
1
1.5
ELLIPTICITY

Fig. 6

FIGURE CAPTIONS

FIG. 1. Magnetic energy distribution among the poloidal Fourier components of the n = 2 tearing mode. This corresponds to the equilibrium sequence of Fig. 4a with $\lambda = 4$.

FIG. 2. Linear growth rate of the n = 1 mode as a function of $S^{-1/3}$.

FIG. 3. Linear growth rate of the n = 1 tearing mode and q(1) value versus ellipticity for the constant-J_ζ equilibrium sequence described in the text.

FIG. 4. (a) Linear growth rate of the n = 1 and n = 2 tearing modes for constant-q equilibrium sequences with $\lambda = 2$ (---) and $\lambda = 4$ (——) described in the text. (b) Saturated island width of the 2;1 and 3;2 helicities for the constant-q sequence with $\lambda = 1.75$.

FIG. 5. (4;1) Fourier component of the n = 1 mode obtained with the initial value code (——) and with the Δ' solver (---).

FIG. 6. (a) Relative change of the linear growth rate of the n = 1 mode obtained with the initial value code (.) and the Δ' solver (o) for the same constant-q equilibrium sequence. (b) Change of Δ' with ellipticity (——) compared with the change of Δ' when only the modification of the equilibrium is taken into account (---).